

Self-Assembled Monolayers Composed of Aromatic Thiols on Gold: Structural Characterization and Thermal Stability in Solution

Nupur Garg, Edwin Carrasquillo-Molina, and T. Randall Lee*

Department of Chemistry, University of Houston, Houston, Texas 77204-5003

Received October 9, 2001. In Final Form: December 19, 2001

Self-assembled monolayers (SAMs) derived from 1,2-bis(mercaptomethyl)-4,5-dialkylbenzene (**1**), 1-mercaptomethyl-3,4-dialkylbenzene (**2**), 1-mercaptomethyl-4-alkylbenzene (**3**), 1-mercapto-4-alkylbenzene (**4**), and 4-mercaptomethyl-4'-alkoxybiphenyl (**5**) were prepared by adsorption from solution onto evaporated gold. The SAMs were characterized by contact angle goniometry, optical ellipsometry, and polarization modulation infrared reflection absorption spectroscopy. Comparison of SAMs generated from **1** and **2** to well-known SAMs generated from normal alkanethiols (**6**) revealed that the former SAMs are densely packed and highly oriented. The alkyl chains of the SAMs derived from **1** and **2** are, however, less crystalline (i.e., less conformationally ordered) than those derived from **6**. The adsorption of compounds **3**, **4**, and **5** onto gold yielded highly crystalline SAMs. Solution-phase thermal desorption of SAMs **1–6** at temperatures ranging from 60 to 110 °C was monitored using ex situ ellipsometry. The desorption profiles of SAMs derived from **1–6** revealed two distinct kinetic regimes: a fast initial desorption followed by a substantially slower desorption. The rates of film desorption in both regimes were observed to increase with increasing temperature. Comparison of the desorption profiles of SAMs **1–6** showed that the structure of the adsorbate strongly influenced the rate of desorption; the differences were more apparent during the advanced stages of desorption. These studies provided a framework for evaluating the structural features and the mechanistic pathways that dictate the thermal stability of SAMs on gold.

Introduction

Self-assembled monolayers (SAMs) of alkanethiols on metal surfaces have enjoyed a relatively brief but distinguished history.¹ These well-organized organic thin films afford control over a wide range of interfacial properties, including wettability,^{2–4} mechanical adhesion,⁵ friction,^{6–9} and protection against corrosion.^{10,11} SAMs on gold have drawn particular interest because of their ease of handling and characterization; moreover, they exhibit moderate stability at room temperature.¹² Studies have shown, however, that SAMs on gold decompose rapidly at elevated temperatures.^{13–15} The lability of these films has been further demonstrated by their exchange with alkanethiols in solution.^{14,16,17} For many applications, the thermal and/or long-term stability of

SAMs is required.¹⁸ Previous strategies designed to promote SAM stability include the use of adsorbates that employ multiple gold–sulfur interactions,^{19–21} intermolecular hydrogen bonding,²² polymerization within the monolayer,^{23–25} and the incorporation of aromatic moieties.^{26–31} Underpotential deposition of a single monolayer of metal onto the surface of gold has also been used to enhance the stability of SAMs.³²

To further these efforts, we have been exploring the use of specifically designed organosulfur moieties that can

- (1) Ulman, A. *Chem. Rev.* **1996**, *96*, 1533.
- (2) Dubois, L. H.; Zegarski, B. R.; Nuzzo, R. G. *J. Am. Chem. Soc.* **1990**, *112*, 570.
- (3) Kang, J. F.; Jordan, R.; Ulman, A. *Langmuir* **1998**, *14*, 3983.
- (4) Shon, Y.-S.; Lee, S.; Colorado, R., Jr.; Perry, S. S.; Lee, T. R. *J. Am. Chem. Soc.* **2000**, *122*, 7556.
- (5) Chaudhury, M. K.; Whitesides, G. M. *Science* **1992**, *255*, 1230.
- (6) Kim, H. I.; Graupe, M.; Oluba, G.; Koini, T.; Imaduddin, S.; Lee, T. R.; Perry, S. S. *Langmuir* **1999**, *15*, 3179.
- (7) Mowery, M. D.; Kopta, S.; Ogletree, D. F.; Salmeron, M.; Evans, C. E. *Langmuir* **1999**, *15*, 5118.
- (8) Lee, S.; Shon, Y.-S.; Lee, T. R.; Perry, S. S. *Thin Solid Films* **2000**, *358*, 152.
- (9) S. Lee; Y.-S. Shon; R. Colorado, Jr.; R. L. Guenard; T. R. Lee; S. S. Perry, *Langmuir* **2000**, *16*, 2220.
- (10) Jennings, G. K.; Laibinis, P. E. *J. Am. Chem. Soc.* **1997**, *119*, 5208.
- (11) Zamborini, F. P.; Campbell, J. K.; Crooks, R. M. *Langmuir* **1998**, *14*, 640.
- (12) Bain, C. D.; Troughton, E. B.; Tao, Y.-T.; Evall, J.; Whitesides, G. M.; Nuzzo, R. G. *J. Am. Chem. Soc.* **1989**, *111*, 321.
- (13) Delamarche, E.; Michel, B.; Kang, H.; Gerber, Ch. *Langmuir* **1994**, *10*, 4103.
- (14) Benesebaa, F.; Ellis, T. H.; Badia, A.; Lennox, R. B. *Langmuir* **1998**, *14*, 2361.
- (15) Tam-Chang, S.-W.; Biebuyck, H. A.; Whitesides, G. M.; Jeon, N.; Nuzzo, R. G. *Langmuir* **1995**, *11*, 4371.

- (16) Biebuyck, H. A.; Bain, C. D.; Whitesides, G. M. *Langmuir* **1994**, *10*, 1825.
- (17) Swalen, J. D.; Allara, D. L.; Andrade, J. D.; Chandross, E. A.; Garoff, S.; Israelachvili, J.; McCarthy, T. J.; Murray, R.; Pease, R. F.; Rabolt, J. F.; Wynne, K. J.; Yu, H. *Langmuir* **1987**, *3*, 932.
- (18) Fukushima, H.; Seki, S.; Nishikawa, T.; Takiguchi, H.; Tamada, K.; Abe, K.; Colorado, Jr., R.; Graupe, M.; Shmakova, O. E.; Lee, T. R. *J. Phys. Chem. B* **2000**, *104*, 7417.
- (19) Whitesell, J. K.; Chang, H. K. *Science* **1993**, *261*, 73.
- (20) Wooster, T. T.; Gamm, P. R.; Geiger, W. E.; Oliver, A. M.; Black, A. J.; Craig, D. C.; Paddon-Row, M. N. *Langmuir* **1996**, *12*, 6616.
- (21) Zhang, H.; Xia, H.; Li, H.; Liu, Z. *Chem. Lett.* **1997**, 722.
- (22) Clegg, R. S.; Reed, S. M.; Hutchison J. E. *J. Am. Chem. Soc.* **1998**, *120*, 2486.
- (23) Kim, T.; Chan, K. C.; Crooks, R. M. *J. Am. Chem. Soc.* **1997**, *119*, 189.
- (24) Ford, J. F.; Vickers, T. J.; Mann, C. K.; Schlenoff, J. B. *Langmuir* **1996**, *12*, 1944.
- (25) Cai, M.; Mowery, M. D.; Menzel, H.; Evans, C. E. *Langmuir* **1999**, *15*, 1215.
- (26) Chang, S.-C.; Chao, I.; Tao, Y.-T. *J. Am. Chem. Soc.* **1994**, *116*, 6792.
- (27) Tour, J. M.; Jones, L., II.; Pearson, D. L.; Lamba, J. J. S.; Burgin, T. P.; Whitesides, G. M.; Allara, D. L.; Parikh, A. N.; Atre, S. V. *J. Am. Chem. Soc.* **1995**, *117*, 9529.
- (28) Dhirani, A.-A.; Zehner, R. W.; Hsung, R. P.; Guyot-Sionnest, P.; Sita, L. R. *J. Am. Chem. Soc.* **1996**, *118*, 3319.
- (29) Tao, Y.-T.; Wu, C.-C.; Eu, J.-Y.; Lin, W.-L. *Langmuir* **1997**, *13*, 4018.
- (30) S. W. Han; Kim, C. H.; Hong, S. H.; Chung, Y. K.; Kim, K. *Langmuir* **1999**, *15*, 1579.
- (31) Kang, J. F.; Ulman, A.; Liao, S.; Jordan, R. *Langmuir* **1999**, *15*, 2095.
- (32) Jennings, G. K.; Laibinis, P. E. *Langmuir* **1996**, *12*, 6173.

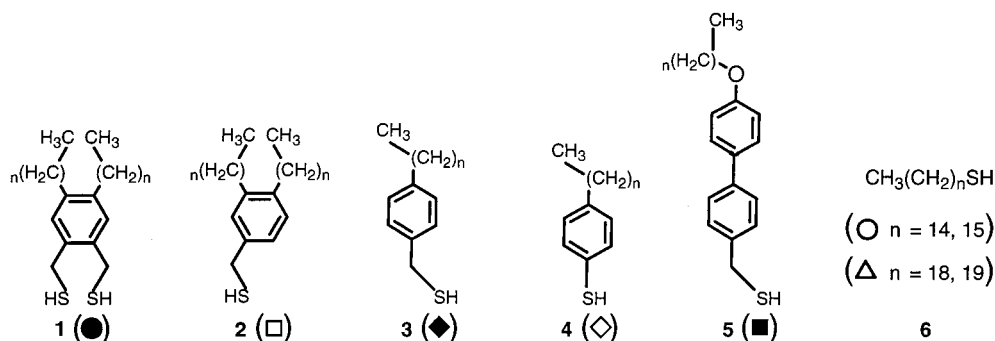
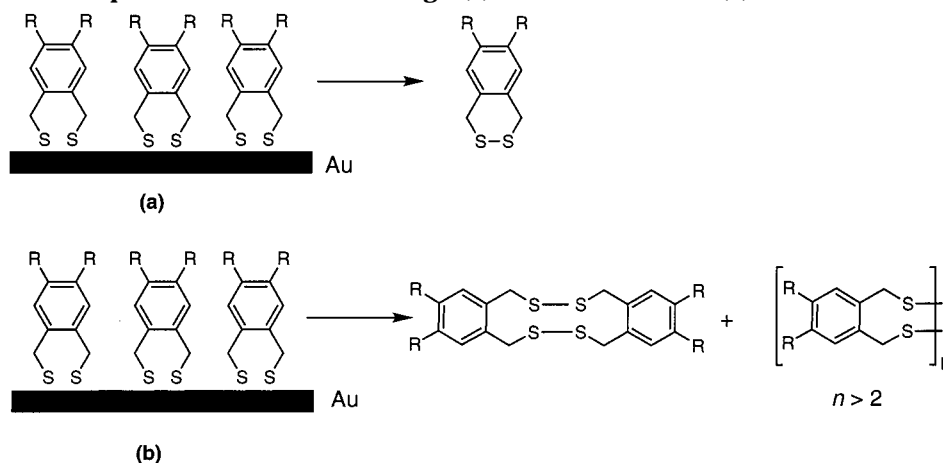


Figure 1. Structures of aromatic-based thiols used for generating SAMs on gold, where the chain lengths are as indicated: **1** ($n = 14, 15$), **2** ($n = 15$), **3** ($n = 14, 15$), **4** ($n = 14, 15$), **5** ($n = 15$), and **6** ($n = 14, 15, 18, 19$).

Scheme 1. Desorption of 1 from Gold through (a) Intramolecular or (b) Intermolecular Pathways



chelate to the surface of gold.^{33–41} One of our strategies utilizes derivatives of 1,2-bis(mercaptomethyl)-4,5-dialkylbenzene (**1**), which are shown in Figure 1.^{33,36,41} As part of our continued interest in studying the structure and properties of these aromatic dithiol-based SAMs,⁴² we report here an investigation of the thermal stability of these new films by performing solution-phase desorption studies in which we monitor the changes in film thickness by ellipsometry. These studies were motivated by three factors that led us to believe that this new class of aromatic dithiol would provide SAMs with enhanced stability. First, the two proximal thiol groups in **1** provide dual bonding moieties for attachment to the surface. Multiple sulfur ligands are known to promote the stability of sulfur-tethered films;⁴³ furthermore, studies of homogeneous organometallic complexes have shown that their stabilities are enhanced by the entropy-driven “chelate effect”.⁴⁴ Second, since literature studies indicate that long chain normal alkanethiols desorb as disulfides from the surface

of gold,^{45,46} the desorption of the new chelating dithiols should be at least partially retarded by ring strain created in forming the cyclic disulfide desorption product (Scheme 1a).⁴⁷ Moreover, desorption pathways involving the formation of intermolecular disulfides are probably untenable, given that these pathways would require the concurrent desorption of four or more tethered sulfur atoms (Scheme 1b). Third, additional stability might be afforded by π -stacking of the aromatic rings within the film.²⁶

Various solution-phase and ultrahigh vacuum (UHV) desorption studies have explored the details of the adsorption and desorption processes of SAMs on gold. The majority of the work to date has been limited to studies of SAMs derived from normal alkanethiols.^{12,32,43,45,46,48} Although many aspects of the desorption mechanism(s) can be inferred from these available literature studies, a detailed examination of the influence of structural variations on the desorption of SAMs has yet to appear. To obtain a more complete understanding of the desorption mechanism(s), we wished to examine the desorption of SAMs having a variety of S–Au bonding motifs and intermolecular interactions.⁴⁰

We report here the desorption of a series of SAMs containing both n -alkyl and n -alkyl aromatic groups and explore the influence of structural variation (see Figure 1) on the rate of desorption. For the purpose of comparison,

(33) Garg, N.; Lee, T. R. *Langmuir* **1998**, *14*, 3815.
 (34) Colorado, R., Jr.; Villazana, R. J.; Lee, T. R. *Langmuir* **1998**, *14*, 6337.
 (35) Shon, Y.-S.; Lee, T. R. *Langmuir* **1999**, *15*, 1136.
 (36) Shon, Y.-S.; Garg, N.; Colorado, R., Jr.; Villazana, R. J.; Lee, T. R. *Mater. Res. Soc. Symp. Proc.* **1999**, *576*, 183.
 (37) Shon, Y.-S.; Colorado, R., Jr.; Williams, C. T.; Bain, C. D.; Lee, T. R. *Langmuir* **2000**, *16*, 541.
 (38) Shon, Y.-S.; Lee, S.; Perry, S. S.; Lee, T. R. *J. Am. Chem. Soc.* **2000**, *122*, 1278.
 (39) Shon, Y.-S.; Lee, T. R. *J. Phys. Chem. B* **2000**, *104*, 8182.
 (40) Shon, Y.-S.; Lee, T. R. *J. Phys. Chem. B* **2000**, *104*, 8192.
 (41) Garg, N.; Friedman, J. M.; Lee, T. R. *Langmuir* **2000**, *16*, 4266.
 (42) See also: Kim, C. H.; Han, S. W.; Ha, T. W.; Kim, K. *Langmuir* **1999**, *15*, 8399.
 (43) Schlenoff, J. B.; Li, M.; Ly, H. *J. Am. Chem. Soc.* **1995**, *117*, 12528.
 (44) See, for example: Purcell, K. F.; Kotz, J. C. *Inorganic Chemistry*; W. B. Saunders: Philadelphia, PA, 1977; pp 739–741.

(45) Nishida, N.; Hara, M.; Sasabe, H.; Knoll, W. *Jpn. J. Appl. Phys.* **1996**, *35*, L 799.
 (46) Nuzzo, R. G.; Zegarski, B. R.; Dubois, L. H. *J. Am. Chem. Soc.* **1987**, *109*, 733.
 (47) Burns, J. A.; Whitesides, G. M. *J. Am. Chem. Soc.* **1990**, *112*, 6296.
 (48) Lavrich, D. J.; Wetterer, S. M.; Bernasek, S. L.; Scoles, G. *J. Phys. Chem. B* **1998**, *102*, 3456.

the number of carbon atoms in the alkyl chains (i.e., the tail groups) was held constant for each type of adsorbate. The nature of the headgroup (i.e., the portion of the adsorbate near the surface of gold) was, however, systematically varied as shown in Figure 1. Compound **1**, for example, contains a dithiol aromatic headgroup rather than the monothiol aromatic headgroup in **2**. Compound **3**, on the other hand, contains a mercaptomethylbenzene headgroup rather than the thiophenol headgroup in **4**. By comparison of the desorption behavior of SAMs derived from **1** and **2**, the influence of dual surface attachment (i.e., chelation) upon film stability can be directly evaluated. Moreover, since attachment via the thiophenol moiety in **4** differs chemically from attachment via the mercaptomethyl moieties in **1**, **2**, and **3**,^{26,29,49} a close examination of the desorption of SAMs derived from **1**, **2**, **3**, and **4** should lend insight regarding the relationship(s) between SAM stability and the nature of the S–Au interaction. Further comparison to monolayers derived from biphenyl-containing **5**²⁶ and normal alkanethiols **6** explores the contribution of π -stacking toward film stability. These studies thus provide the basis for a more complete understanding of the relationships between structure and stability of SAMs on gold.

Experimental Section

Preparation and Analysis of SAMs. The experimental procedures and techniques used to generate and characterize the SAMs have been described in previous reports^{33–41} and are included here as Supporting Information. Methods for the synthesis of the aromatic thiols are also provided as Supporting Information. Experimental details of the thermal desorption studies are given in the following paragraph.

Thermal Desorption Experiments. SAM-coated gold wafers were immersed in approximately 100 mL of solvent (isooctane or decalin) that was maintained at a constant temperature ranging from 60 to 110 °C with an accuracy of ± 1 °C. The wafers were removed at selected intervals of time, rinsed with ethanol, and blown dry with ultrapure nitrogen. Ellipsometric thicknesses were measured immediately, and the wafers were then reimmersed in the heated bath.⁵⁰ For each measurement, the data were collected from three separate spots per slide.

Results

1. Thicknesses and Wettabilities. The ellipsometric thicknesses and contact angle wettabilities of the SAMs generated from the 1,2-bis(mercaptomethyl)-4,5-dialkylbenzenes (**1**), 1-mercaptomethyl-3,4-dihexadecylbenzene (**2**), 1-mercaptomethyl-4-alkylbenzenes (**3**), and 1-mercapto-4-alkylbenzenes (**4**), where $n = 14$ and 15, were similar to those of the corresponding normal alkanethiols (**6**), where $n = 14$ and 15 (Table 1). These observations suggest that the aromatic thiols generate well-packed SAMs on gold with the expected orientation. The fact that these data are indistinguishable from those measured on the SAMs derived from normal alkanethiols suggests that the differing nature of the headgroups of these adsorbates (i.e., chelating and single attachment) plays no strong role in influencing the structural and interfacial properties of the films. The thickness and wettability data of the SAM derived from the 4-mercaptomethyl-4'-hexadecan-oxylbiphenyl (**5**) are also consistent with a well-packed SAM on gold with the expected orientation (Table 1). The data collected here agree well with those reported previ-

Table 1. Ellipsometric Thicknesses, Advancing Contact Angles of Water (H₂O) and Hexadecane (HD), and $\nu_a^{\text{CH}_2}$ Band Positions of SAMs Derived from 1–6^a

compd	thickness (Å)		$\theta_a^{\text{H}_2\text{O}}$ (deg)		θ_a^{HD} (deg)		$\nu_a^{\text{CH}_2}$ (cm ⁻¹)
	$n = 14$	$n = 15$	$n = 14$	$n = 15$	$n = 14$	$n = 15$	
1	25	27	115	115	49	49	2922
2		26		115		50	2921
3	23	24	113	113	54	47	2919
4	20	21	113	113	51	46	2920
5		33		113		55	2919
6	24	25	115	115	49	49	2919

^a The thicknesses were reproducible within ± 2 Å. The average contact angles of water and hexadecane were reproducible within $\pm 2^\circ$. The $\nu_a^{\text{CH}_2}$ band positions were reproducible within ± 1 cm⁻¹.

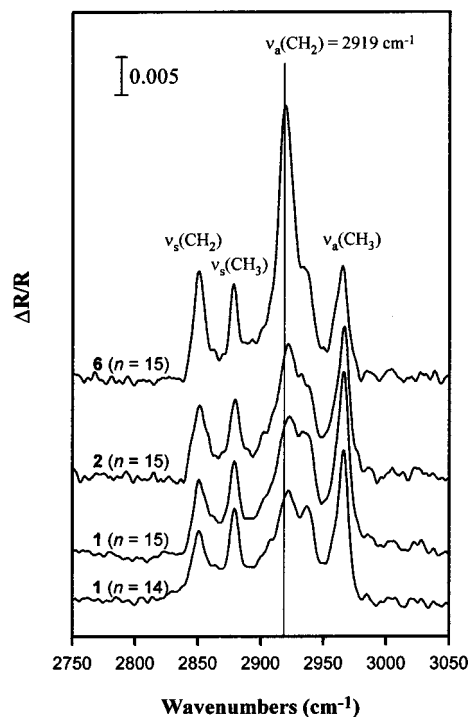


Figure 2. Surface infrared spectra (PM-IRRAS) of SAMs generated from **1** ($n = 14, 15$), **2** ($n = 15$), and **6** ($n = 15$) on gold. The vertical marker for the $\nu_a^{\text{CH}_2}$ band is positioned at 2919 cm⁻¹ to facilitate comparison of the data.

ously by Tao and co-workers using this adsorbate to generate SAMs on gold.²⁶

For the SAMs derived from **3** and **4**, the ellipsometric data showed no unanticipated trends, but the contact angles of hexadecane exhibited an unusually strong dependence on the lengths of the hydrocarbon chains (i.e., the contact angles varied by 5–7° for odd and even chain lengths). This type of “odd–even” or “parity” effect has been observed in several SAM systems.^{26,34,51} The wetting properties of hydrocarbon liquids such as hexadecane are particularly sensitive to fine differences in structure and orientation of the top 2–3 Å of hydrocarbon SAMs; lower contact angles of hexadecane are observed when the terminal methyl groups tilt away from the surface normal, exposing the more wettable methylene moieties.⁴

2. Characterization by Polarization Modulation Infrared Reflection Absorption Spectroscopy (PM-IRRAS). Chelating Aromatic Dialkyl Dithiols 1. Figure 2 shows the PM-IRRAS spectra of the SAMs derived from compounds **1**, **2**, and **6** ($n = 15$). In SAMs on gold

(49) Jung, H. H.; Won, Y. D.; Shin, S.; Kim, K. *Langmuir* **1999**, *15*, 1147.

(50) We observed little or no differences in thicknesses of the desorbed monolayers when we used reimmersed SAM-coated wafers or when we used SAM-coated wafers that were freshly withdrawn from solution at the indicated intervals of time.

(51) Graupe, M.; Takenaga, M.; Koini, T.; Colorado, R., Jr.; Lee, T. *J. Am. Chem. Soc.* **1999**, *121*, 3222.

derived from normal alkanethiols, the alkyl chains adopt a predominantly trans zigzag conformation.¹ The frequency and intensity of the methylene antisymmetric C–H stretch, $\nu_a^{\text{CH}_2}$, are particularly sensitive to the degree of conformational order (or crystallinity) of the films.⁵² The monolayer films derived from **1** exhibit a $\nu_a^{\text{CH}_2}$ band at 2922 cm^{-1} , which is 3–4 cm^{-1} higher than that typically observed for highly crystalline SAMs on gold. The shift of the $\nu_a^{\text{CH}_2}$ band to higher frequency suggests that the monolayers derived from **1** contain gauche defects.⁵³ The ratio of intensities of the $\nu_a^{\text{CH}_2}$ and $\nu_s^{\text{CH}_2}$ bands can also be used to characterize the tilt and the twist of the alkyl chains of SAMs.^{52,53} Figure 2 shows that the observed ratio of band intensities (i.e., $\nu_a^{\text{CH}_2}/\nu_s^{\text{CH}_2}$) is noticeably smaller for the chelating SAMs derived from **1** than for the normal SAM derived from **6**. These data suggest that the chelating SAMs exhibit unique chain twist and/or chain tilt when compared to normal SAMs on gold.^{54–58} These differences might arise from the introduction of the tetrasubstituted benzene moiety, which can plausibly impose structural constraints and/or alter the energetics of the interchain interactions in the chelating SAMs. Future studies will address these structural issues in greater detail.

Measurements by PM-IRRAS can also be used to evaluate the orientation of the terminal methyl group in hydrocarbon SAMs.^{52,53} For SAMs on gold derived from normal alkanethiols, the ratio of the intensities of the symmetric ($\nu_s^{\text{CH}_3} \sim 2878 \text{ cm}^{-1}$) and the antisymmetric ($\nu_a^{\text{CH}_3} \sim 2965 \text{ cm}^{-1}$) methyl bands is known to change systematically with the terminal methyl group orientation, which is governed by the odd vs even length of the underlying methylene chain.^{28,59} For SAMs derived from the chelating dithiols **1**, however, the ratio of the intensities of these two bands is roughly constant for both odd and even chain lengths (Figure 2). Similarly, no odd–even effects were observed in measurements of wettability on these SAMs (see Table 1 and ref 33). Both the PM-IRRAS and the wettability data are consistent with a model in which the chelating SAMs possess less-ordered (or perhaps differently oriented) tail groups when compared to SAMs derived from normal alkanethiols.

(52) Allara, D. L. In *Characterization of Organic Thin Films*; Ulman, A., Ed.; Butterworth-Heinemann: Boston, MA, 1995; pp 57–86.

(53) Anderson, M. R.; Evanaik, M. N.; Zhang, M. *Langmuir* **1996**, *12*, 2337.

(54) While a quantitative structural analyses (i.e., chain tilt and twist) of organic films deposited on metal surface can be obtained from the band intensities of normalized PM-IRRAS spectra, extensive modeling, data analysis, and data manipulation are required.^{52,55} In the preliminary IR studies reported here, we use raw PM-IRRAS data to provide only a qualitative comparison of the band intensities within the spectrum of a single sample.

(55) Buffeteau, T.; Desbat, B.; Turlet, J. M. *Appl. Spectrosc.* **1991**, *45*, 380.

(56) In addition to the intensities of the methylene stretching bands, measurements of ellipsometric thickness might also be expected to reflect the degree of tilt of the alkyl chains of SAMs. Since, however, the thicknesses of the films derived from **1** are within $\pm 1 \text{ \AA}$ of the films derived from the corresponding normal alkanethiols **6** (Table 1),³³ the ellipsometric data fail to indicate any differences in the tilt angles of these two types of SAMs. We note, however, that the SAMs derived from **1** possess gauche defects (vide supra) and that normal alkanethiol SAMs on gold are known to tilt approximately 30° from the surface normal.¹ Since the presence of gauche defects can effectively reduce the total length of an alkyl chain by approximately one carbon atom (compared to an all-trans extended chain),^{57,58} the presence of gauche defects, when coupled with a less tilted orientation, might give rise to indistinguishable ellipsometric thicknesses for SAMs derived from **1** and **6**.

(57) Kim, Y.; Strauss, H. L.; Snyder, R. G. *J. Phys. Chem.* **1988**, *92*, 5080.

(58) Maroncelli, M.; Strauss, H. L.; Snyder, R. G. *J. Chem. Phys.* **1985**, *82*, 2811.

(59) Nuzzo, R. G.; Dubois, L. H.; Allara, D. L. *J. Am. Chem. Soc.* **1990**, *112*, 558.

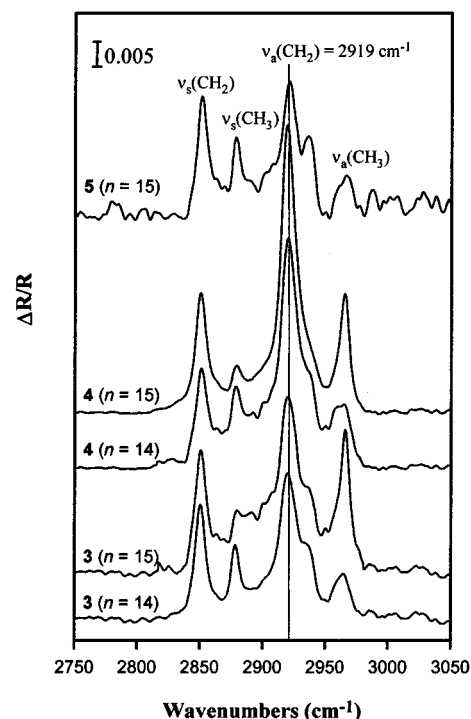


Figure 3. Surface infrared spectra (PM-IRRAS) of SAMs generated from **3** ($n = 14, 15$), **4** ($n = 14, 15$), and **5** ($n = 15$) on gold. The vertical marker for the $\nu_a^{\text{CH}_2}$ band is positioned at 2919 cm^{-1} to facilitate comparison of the data.

Aromatic Dialkyl Monothiol 2. The data in Figure 2 and Table 1 show that the SAM derived from **2** exhibits a $\nu_a^{\text{CH}_2}$ band at 2921 cm^{-1} , which is indistinguishable from that of the SAMs derived from **1** ($n = 14$ and 15). Because lateral diffusion of monothiol **2** is probably more facile than that for **1** (due to the chelating nature of the latter) and the lengths of the alkyl chains of both types of adsorbates are similar, it seems plausible that the alkyl chains in monolayers derived from **2** can achieve crystallinities similar to those of the monolayers derived from **1**.

Aromatic Monoalkyl Monothiols 3 and 4. As judged by the $\nu_a^{\text{CH}_2}$ band positions, compounds **3** and **4** generate highly ordered monolayers on gold (Figure 3, Table 1). To confirm the origin of the odd vs even wettability effects observed for these SAMs (vide supra), we examined the intensities of the methyl vibrational modes,^{52,53} which are known to vary with the orientation of the terminal methyl group in normal alkanethiol SAMs on gold.^{4,26,59} Figure 3 shows that for $n = 14$, the $\nu_a^{\text{CH}_3}$ band and the $\nu_s^{\text{CH}_3}$ band exhibit approximately equal intensities; conversely, for $n = 15$, the $\nu_a^{\text{CH}_3}$ band is substantially more intense than the $\nu_s^{\text{CH}_3}$ band. As observed by Tao and co-workers for monolayers derived from **5** and related adsorbates,²⁶ the odd–even variation in intensity observed for adsorbates **3** and **4** is more pronounced than that observed for normal alkanethiols on gold.⁵⁹ The enhanced odd–even variation suggests that the alkyl chains in SAMs derived from **3** and **4** are oriented differently than those of normal alkanethiol-based SAMs. It seems plausible that the introduction of the phenyl ring could impose structural constraints and/or alter the energetics of the interchain interactions leading to differences in chain twist and chain tilt.

Biphenyl Monoalkyl Monothiol 5. Figure 3 shows the PM-IRRAS spectrum of the SAM derived from 4-mercaptomethyl-4'-hexadecanobiphenyl (**5**). The spectrum shows a $\nu_a^{\text{CH}_2}$ band at 2919 cm^{-1} , which suggests

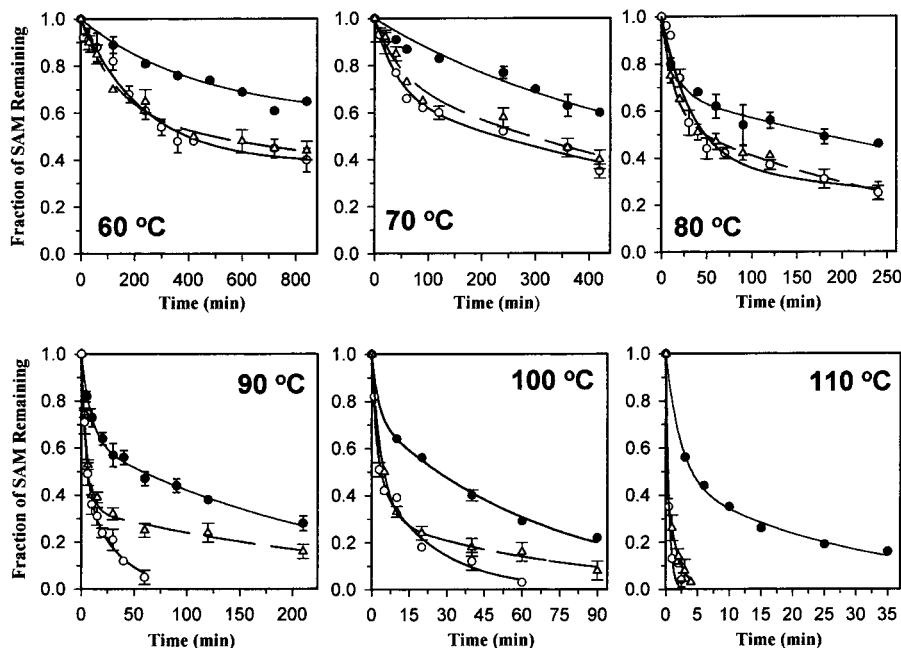


Figure 4. Desorption profiles of SAMs derived from chelating dithiols **1** (filled circles, $n = 15$) and normal alkanethiol **6** (hollow circles, $n = 15$; hollow triangles, $n = 19$) at temperatures ranging from 60 to 110 °C in decalin. The solid and the dashed lines are used simply to guide the eye. Where error bars are omitted, the standard deviation was equal to or smaller than the size of the symbol.

that this adsorbate forms a highly crystalline monolayer on gold. The data obtained here are consistent with those reported by Tao and co-workers.²⁶

Summary of the $\nu_a^{\text{CH}_2}$ Band Positions for All Adsorbates. Table 1 provides a summary of the $\nu_a^{\text{CH}_2}$ band positions observed for the SAMs derived from adsorbates **1–6**. On the strict basis of the frequency value, the data suggest the following general trend in the degree of crystallinity of the alkyl chains of the SAMs: **1–2** < **3–6**. Since the crystallinities of **3–6** are indistinguishable, we conclude that the relatively low crystallinities of the SAMs derived from **1** and **2** arise from factors other than interchain steric hindrance between adjacent aromatic moieties. It seems plausible, however, that the relative orientation of the benzylic carbon atoms in **1**, which are necessarily directed away from each other by the geometry of the aromatic ring, introduces steric hindrance that prevents closest packing of the alkyl chains.

3. Thermal Desorption Studies. General Methods and Observations. We evaluated the thermal stabilities of the SAMs derived from **1–6** by ex situ monitoring of their desorption into a contacting hydrocarbon solvent. Specifically, the desorption studies were performed by placing SAM-coated wafers into stirred solutions of either isooctane or decalin at temperatures ranging from 60 to 110 °C. We chose these solvents to discourage intercalation of the solvent into the monolayer. The extent of desorption was monitored by examining the change in ellipsometric thickness.^{60,61}

Figures 4–6 show the desorption profiles of the SAMs generated from the aromatic-based thiols **1–5** ($n = 15$)

and the corresponding normal alkanethiols **6**. The desorption data of all of the SAMs share at least three common features. First, the data exhibit two distinguishable kinetic regimes of desorption: a fast initial regime followed by a substantially slower or nondesorbing regime. Second, the rate and/or extent of desorption in both regimes increases with increasing temperature. Third, the relative rates of desorption in both regimes are influenced by the nature of the adsorbate. Figure 4 readily illustrates all three trends. The desorption profiles of **1** and **6** exhibit two kinetic regimes at all temperatures as judged by the appearance of two distinctly different slopes in the plots. The data also show enhanced desorption of both types of adsorbates at higher temperatures. Further, at all times, the fraction of the chelating SAM remaining on the surface was higher than that of the normal SAM, suggesting that the structural nature of the adsorbate influences the rate of desorption in both kinetic regimes.

To establish that the fractional coverages measured by ellipsometry correspond to residual organosulfur adsorbates rather than surface contaminants, we analyzed partially desorbed SAMs derived separately from **1** and **6** by PM-IRRAS and X-ray photoelectron spectroscopy (XPS) (data not shown). We collected these data from samples desorbed at 100 °C in decalin at the point at which the fractional coverage remaining was $\sim 25\%$ for each adsorbate as judged by ellipsometry (i.e., clearly within the slow/nondesorbing regimes of both adsorbates). While the $\nu_a^{\text{CH}_3}$ bands in the PM-IRRAS spectra were qualitatively less intense than those collected at full coverage, their ready observation was consistent with the presence of a partially adsorbed monolayer rather than adsorbed contaminants. Moreover, the shift to higher wavenumber of the $\nu_a^{\text{CH}_2}$ band was consistent with the expected decrease in crystallinity for partially desorbed SAMs. Analyses by XPS provided further support for partial SAM desorption by indicating the presence of carbon, bound sulfur,⁶² and a trace of oxygen on the surface of gold.⁶³ Moreover, the

(60) A potential drawback of this approach centers on the fact that ellipsometric measurements of partial monolayers might fail to vary linearly with the amount of adsorbed material since the optical constants of the films can plausibly vary with changes in coverage. This constraint, when coupled with the inherent experimental error in routine measurements of ellipsometric thickness, prevented us from performing a meaningful kinetic analysis of the desorption profiles from beginning to end (vide infra). We note, however, that other researchers have reliably used ellipsometry as the primary analytical tool for monitoring the desorption behavior of organic thin films.^{12,32,61}

(61) Gun, J.; Sajiv, J. *J. Colloid Interface Sci.* **1986**, *112*, 457.

(62) Castner, D. G.; Hinds, K.; Grainger, D. W. *Langmuir* **1996**, *12*, 5083.

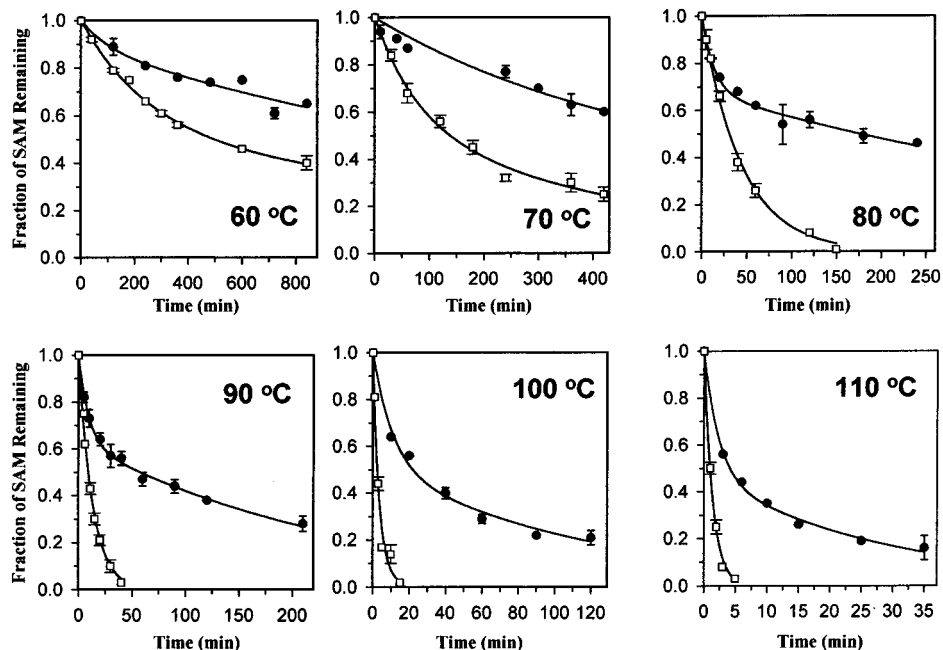


Figure 5. Desorption profiles of SAMs derived from chelating dithiols **1** (filled circles; $n = 15$) and dialkyl monothiol **2** (hollow squares) at temperatures ranging from 60 to 110 °C in decalin. The solid and the dashed lines are used simply to guide the eye. Where error bars are omitted, the standard deviation was equal to or smaller than the size of the symbol.

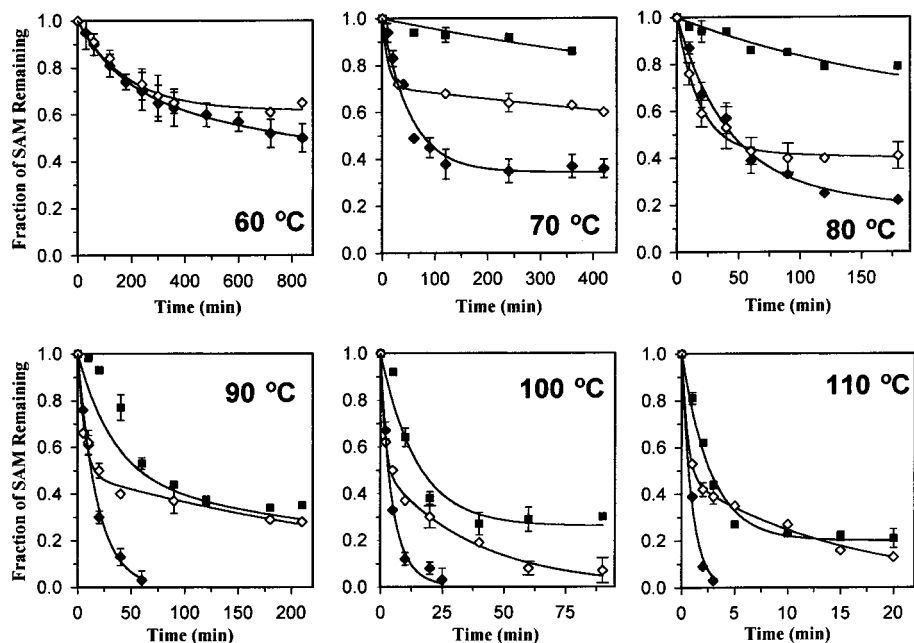


Figure 6. Desorption profiles of SAMs derived from 1-mercaptomethyl-4-alkylbenzene **3** (filled diamonds; $n = 15$), 1-mercapto-4-alkylbenzene **4** (hollow diamonds; $n = 15$), and 1-mercaptomethyl-4'-alkylbiphenyl **5** (filled squares) at temperatures ranging from 60 to 110 °C in decalin. The solid and the dashed lines are used simply to guide the eye. Where error bars are omitted, the standard deviation was equal to or smaller than the size of the symbol.

S/Au ratio decreased substantially for both adsorbates when compared to that found in XPS data collected at full coverage.

Kinetic Analysis. We analyzed the desorption data in Figures 4–6 by considering the fast and slow/nondesorbing regimes separately. To evaluate the rates of desorption at various temperatures in the fast desorbing regime, we fitted the desorption data to first-order kinetics according to eq 1,¹² where T_0 is the initial thickness of the SAM, T_t

is the thickness of the SAM at time t , and T_∞ is the thickness of the slow/nondesorbing fraction of the SAM. The thicknesses of the fractional SAM remaining were plotted versus time, and the first-order rate constant (k) was derived from the initial slope of the curves at the different temperatures. The activation enthalpies and entropies for desorption were calculated using the Eyring equation (eq 2),⁶⁴

$$(T_t - T_\infty)/(T_0 - T_\infty) = e^{-kt} \quad (1)$$

(63) Lee, M.-T.; Hsueh, C.-C.; Freund, M. S.; Ferguson, G. S. *Langmuir* 1998, 14, 6419.

$$k = k_B T/h e^{-\Delta H^\ddagger/RT} e^{\Delta S^\ddagger/R} \quad (2)$$

where k_B is Boltzmann's constant, h is Planck's constant, ΔH^\ddagger is the enthalpy of activation, and ΔS^\ddagger is the entropy of activation. A plot of $\ln[k(h/k_B T)]$ vs $1/T$ afforded a line with the slope and intercept providing the enthalpies and entropies of activation, respectively. Using the desorption data collected on the SAMs derived from **1** and **6** ($n = 15$), Figure 7 provides illustrative examples of the Eyring plots.

Table 2 summarizes the free energy, enthalpy, and entropy of activation obtained from the Eyring plots of the fast-desorbing regime for the SAMs derived from compounds **1–6** ($n = 15$). The data show no substantial differences; all free energies of activation were 27 ± 1 kcal/mol. The kinetics of desorption, however, were clearly different for the different adsorbates. Table 3 shows the rate constants for desorption in the fast regime at 90 °C for the various SAMs; the relative trends in the rate constants shown here were observed at all temperatures. A comparison of the rate constants shows that the SAM derived from **1** desorbs slower than any other SAM. Also, the aromatic-based SAMs desorb more slowly than the SAM derived from **6**.

To explore the influence of chain length on the stabilities of the SAMs, we compared the desorption profiles of the SAM derived from **1** ($n = 15$) to SAMs derived both from hexadecanethiol and eicosanethiol (see Figure 4). For the hexadecanethiol-based SAM ($n = 15$), the length of the alkyl chain is identical to that standing above the phenyl moiety in the SAM derived from **1**, where $n = 15$ (see Figure 1). In contrast, for the eicosanethiol-based SAM ($n = 19$), the length of the alkyl chain is identical to the number of carbon atoms per chain in the SAM derived from **1**, where $n = 15$ (see Figure 1). The data for the desorption of the SAMs in Figure 4 and Table 4 show that the desorption profiles and the activation energies, respectively, vary little with chain length in the fast desorbing regime.

To probe this issue further, we examined the influence of chain length on the thermal desorption of **1** ($n = 13–16$) and **6** ($n = 16–19$) in isoctane at temperatures ranging from 70 to 90 °C. We note that in comparing these two series of compounds, **1** vs **6**, the overall chain lengths (i.e., the number of carbon atoms along each chain from the sulfur atom to the terminal methyl group) overlap within ± 1 carbon atom. As described above, the desorption data in the fast-desorbing regime were fit to first-order kinetics and evaluated using eq 2. A plot of the enthalpies of activation vs the number of methylene units (Figure 8) shows an increase of 0.6 ± 0.2 kcal/mol per methylene unit for the chelating dithiols **1** and an increase of 0.3 ± 0.2 kcal/mol per methylene unit for the normal alkanethiols **6**. The latter value is consistent with that reported by Bain et al. for the desorption of normal alkanethiolate-based SAMs on gold in isoctane (0.2 kcal/mol per methylene unit).¹²

For the slow/nondesorbing regime, we were unable to perform a quantitative analysis of the kinetic data. The relatively small changes in ellipsometric thickness in this regime were within experimental error and thus not reliably distinguishable. By choosing, however, a set of parameters such as the time required for the desorption of a given percentage of the SAM at a given temperature, a qualitative picture of the desorption tendencies for all adsorbates could be obtained. If we consider, for example,

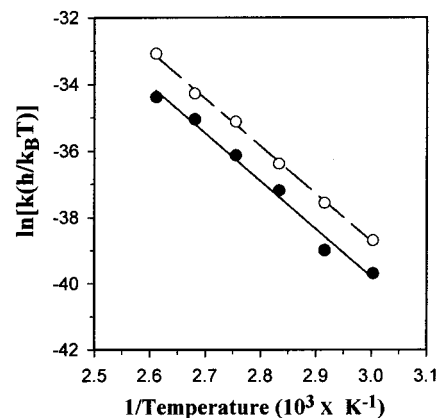


Figure 7. Eyring plots for the desorption of chelating dithiol **1** (filled circles; $n = 15$) and normal alkanethiol **6** (hollow circles; $n = 15$) at temperatures ranging from 60 to 110 °C in decalin.

Table 2. Activation Parameters Evaluated from Eyring Plots of the Data in the Fast-Desorbing Regime for SAMs Derived from 1–6 in Decalin, Where $n = 15$

compd	1	2	3	4	5	6
ΔH^\ddagger ^a	29	29	26	26	26	28
ΔS^\ddagger ^b	7	3	1	1	1	8
ΔG^\ddagger , ^a at 25 °C	27	28	26	26	26	26

^a kcal/mol. ^b cal/(deg mol). Values of ΔG^\ddagger were reproducible within ± 1 kcal/mol for independent runs of a given substrate.

Table 3. First-Order Rate Constants for the Desorption of SAMs Derived from 1–6 in the Fast-Desorbing Regime at 90 °C in Decalin, Where $n = 15$ ^a

	1	2	3	4	5	6
$k \times 10^{-1}$ (min ⁻¹)	0.67	1.0	1.0	1.2	0.90	1.8

^a We estimate the experimental error in the rate constants to be $\pm 15\%$.

the time required for 75% of the monolayer to desorb at 100 °C (Table 5), the SAMs derived from **1** consistently show a greater requisite time interval for desorption than those derived from **2–6**. Moreover, the data in Table 5 for all of the adsorbates suggest the following overall trends in stability for the SAMs: **1** > **5** > **4** > **6** > **3** > **2**.

Discussion

The two-stage desorption profiles observed in the present study are consistent with literature descriptions of distinct kinetic regimes for the desorption of alkanethiolate-based SAMs on polycrystalline gold.⁴³ Furthermore, literature studies of the exchange of adsorbed alkanethiols (R–SH) with structurally different alkanethiols (R'–SH) in solution show two distinct kinetic regimes: a fast initial exchange followed by a substantially slower exchange.^{27,32,40} The fast exchange was initially proposed to occur at defect sites (e.g., domain boundaries, crystal boundaries, steps, or impurities on the underlying gold); more recently, however, Walczak et al. examined the electrochemical reductive desorption of normal alkanethiols on gold.⁶⁵ From these studies, the authors concluded that the alkanethiols desorb from both terrace and step sites with the adsorbate bound at the step sites by approximately 6 kcal/mol more than those bound at the terrace sites. The influence of defect population on desorption was also confirmed by Schlenoff et al.,⁴³ where a faster rate of desorption was found for smaller defect populations. While

(64) See, for example: Lowery, T. H.; Richardson, K. S. *Mechanism and Theory in Organic Chemistry*, 3rd ed.; Harper & Row: New York, 1987; p 209.

(65) Walczak, M. M.; Alves, C. A.; Lamb, B. D.; Porter, M. D. *J. Electroanal. Chem.* **1995**, *396*, 103.

Table 4. Activation Parameters Evaluated from Eyring Plots of the Data in the Fast-Desorbing Regime for SAMs Derived from 1, 3, 4, and 6 in Decalin

	1		3		4		6		
	<i>n</i> = 14	<i>n</i> = 15	<i>n</i> = 19						
ΔH^\ddagger ^a	28	29	26	26	26	26	28	28	29
ΔS^\ddagger ^b	7	7	1	1	1	1	7	8	15
ΔG^\ddagger , ^a at 25 °C	26	27	26	26	26	26	26	26	25

^a kcal/mol. ^b cal/(deg mol). Values of ΔG^\ddagger were reproducible within ± 1 kcal/mol for independent runs of a given substrate.

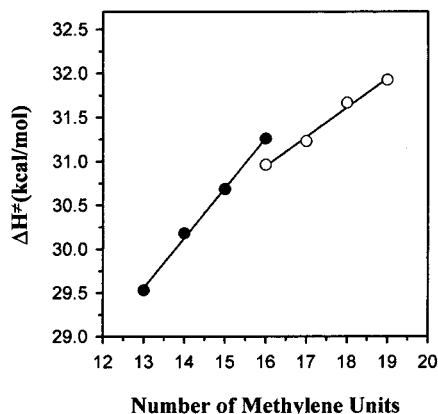
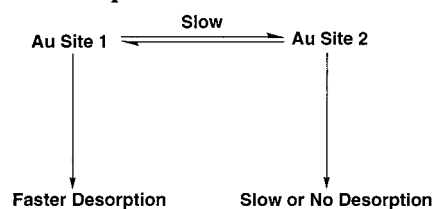


Figure 8. Plots of the enthalpies of activation vs the number of methylene units (*n*) per chain for the desorption of aromatic dithiols **1** (filled circles; *n* = 13–16) and normal alkanethiols **6** (open circles; *n* = 16–19) in isooctane. Slopes of the least-squares fits to these data yield a change in activation enthalpy of 0.6 ± 0.2 and 0.3 ± 0.2 kcal/mol per methylene group, respectively.

Table 5. Time Interval Required for the Desorption of 75% of the Monolayer at 100 °C in Decalin for the SAMs Derived from 1–6, Where *n* = 15

	1	2	3	4	5	6
time (min)	75	<10	10	25	40	15

Scheme 2. Illustration of the Two-Site Model for the Desorption of SAMs from Gold



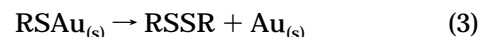
it is likely that multiple distinct binding sites on the surface give rise to distinct desorption regimes for the adsorbates examined in the present work, we believe that other factors might also influence the rates of desorption. Specifically, the fact that we observe differences in the rates of desorption for SAMs generated from **1–6** suggests that structural variations of the adsorbate also influence the desorption behavior of SAMs on gold.

To understand the relative influence of multiple binding sites on the surface and structural variations of the adsorbates, we considered a two-site model of desorption (Scheme 2).^{66,67} In this model, site 1 represents the binding sites on gold where thiols are weakly bound and, consequently, desorb with fast rates from the surface. In

contrast, site 2 represents the binding sites on gold where thiols are strongly bound, and little or no desorption occurs. In the fast-desorbing regime, the structural features of the adsorbates might directly influence the rates of desorption from site 1. In the slow-desorbing regime, however, the thiols adsorbed to site 2 can either directly desorb from site 2 or diffuse to site 1 before desorbing from the surface. In the latter case, the rate of diffusion of the thiolate species might also be strongly influenced by the structural features of the adsorbates.

We readily admit, however, that we cannot exclude the partial influence of diffusional effects in the fast-desorbing regime. Likewise, we cannot exclude the partial influence of direct desorption (i.e., desorption that is reaction-limited rather than diffusion-limited) in the slow/nondesorbing regime. The presently ill-defined nature of both desorption regimes and the poorly understood differences between them preclude a quantitative assessment of the relative contributions of these phenomena in either regime. We find it useful, however, to analyze the data in the fast-desorbing regime in the context of direct (i.e., reaction-limited) desorption and to analyze the data in the slow/nondesorbing regime in the context of indirect (i.e., diffusion-limited) desorption.

Fast-Desorbing Regime: Reaction-Limited Desorption. There is substantial evidence that SAMs derived from normal alkanethiols desorb as disulfides from the surface of gold (eq 3).^{45,46}



The differences in the rates of desorption exhibited by the SAMs derived from **1–6** can be at least partially rationalized by considering disulfide formation to be the rate-determining step in the fast-desorbing regime. In this scenario, the rate of disulfide formation should be predominantly influenced by the difference between the ground-state energy of the adsorbed monolayer and the transition-state energy for the formation of the disulfide. The ground-state energy of the monolayer is determined by a number of factors, such as the strength of the S–Au bond and intermolecular interactions (e.g., van der Waals forces) within the monolayer. While both of these factors are likely to influence the transition-state energy as well, steric factors arising from the approach of the two sulfur headgroups required for disulfide formation might also influence the transition-state energy.

The data in Table 3 show that the chelating SAMs **1** exhibited the slowest rates of desorption in the fast-desorbing regime. Due to ring strain, the formation of a cyclic intramolecular disulfide from **1** (see Scheme 1a) will be energetically disfavored by ~ 2.4 kcal/mol.⁴⁷ Furthermore, the formation of an intermolecular disulfide will be entropically disfavored as it would require the formation of a dimer, trimer, or even larger heterocycle as shown in Scheme 1b. Both of these factors can plausibly contribute to the enhanced stability of the chelating SAMs in the fast-desorbing regime. While one might argue that the relative crystallinities of the SAMs should also

(66) An alternative rationalization for the differences in the desorption profiles of SAMs derived from **1–6** involves differences in the reconstruction of the gold surface upon heating.⁶⁷ Future studies will attempt to distinguish between this and other hypotheses.

(67) Dishner, M. H.; Hemminger, J. C.; Feher, F. J. *Langmuir* **1997**, *13*, 2318.

influence their desorption behavior, the melt transitions in these SAMs most likely occur at temperatures lower than those employed here.⁶⁸ Consequently, we would expect to see no correlation between the desorption behavior and the degree of crystallinity suggested by the PM-IRRAS measurements (vide supra). The data are thus consistent with this assumption: the least crystalline but most stable SAMs are those derived from **1**.

The data in Table 3 also show that the aromatic-based SAMs derived from **2–5** desorb more slowly than the SAMs derived from the normal alkanethiols **6**. The enhanced stability of the SAMs derived from **2–5** can be rationalized on the basis of the following two arguments: (1) favorable π -stacking interactions that lower the ground-state energy for adsorbed **2–5** are lost in the transition state for desorption, and/or (2) steric repulsions between adjacent aromatic rings of **2–5** raise the transition-state barrier for desorption as a disulfide. Within the series of the SAMs derived from **2–5**, the differences in the rate constants for desorption were less than the error associated with their values. Consequently, we can draw no conclusions regarding the relative stabilities of these SAMs in the fast-desorbing regime.

Slow/Nondesorbing Regime: Diffusion-Limited Desorption. As noted above, the rates of desorption in the slow/nondesorbing regime are likely to be strongly influenced by the rate of diffusion of the adsorbates from site 2 to site 1 (see Scheme 2). Differences in the rates of diffusion on the surface can plausibly arise from at least two factors: differences in intermolecular interactions within the SAM (e.g., π -stacking interactions) and/or differences in the nature of the S–Au interaction (e.g., chelation). The data in Table 5 indicate that the SAMs derived from **1** are thermally more robust than those derived from **2–6**. Moreover, the data in Table 3 show that a smaller percentage of the chelating SAM desorbs in the fast-desorbing regime than that of any other SAM. We believe that the enhanced stability of the SAMs derived from **1** in the slow/nondesorbing regime arises predominantly from the chelate effect. Since the chelating dithiol **1** is bound to the surface via two sulfur atoms, diffusion on the surface is restricted because it requires the highly correlated (simultaneous and/or stepwise) movement of two sulfur atoms. In contrast, the adsorbates **2–6** are free from this restriction.

Analysis of the desorption data of the SAMs derived from **3** and **4** suggests that the monolayers generated from **4** are marginally more stable than those generated from **3**. For compound **3**, the sulfur atom is attached to the benzylic position of the aromatic ring. For compound **4**, however, the sulfur atom is attached directly to the aromatic ring. With regard to diffusion limitation, the difference in stability can plausibly arise from the following effect: the thiolate of **4** is more stable and “softer” than the thiolate of **3**, which might correspond to a lower ground-state energy for adsorbed **4** relative to that of **3**. This effect could serve to inhibit the rate of diffusion of **4** to the fast-desorbing sites and, thus, inhibit its rate of desorption from the surface. Reaction limitation, however, might also play a role here. Assuming no differences in the transition-state barriers for the desorption of **3** and **4**, then a lower ground-state energy for adsorbed **4** would correspond to a faster rate of desorption for **3**. On the other hand, since the S–S bond energy in dibenzyl disulfide (68 kcal/mol) is roughly three times that of diphenyl disulfide (26 kcal/mol),⁶⁹ the transition-state barrier for the desorption of

3 is probably lower than that of **4**, which would again suggest an enhanced rate of desorption for **3**.

SAMs derived from **5** are analogous to those derived from **3** with the exception of an additional phenyl ring in the backbones of the chains. Moreover, the data in Table 5 suggest that the SAMs derived from **5** are second only to those derived from **1** with regard to stability. In comparison of the SAMs derived from **3** and **5**, the additional phenyl ring in **5** can plausibly inhibit surface diffusion via enhanced π -stacking and/or enhanced steric interaction mechanisms. As outlined above, the inhibition of diffusion on the surface should correlate with an enhanced stability for SAMs in the slow/nondesorbing regime. If we consider reaction limitation, the increased π -stacking due to the additional phenyl ring in **5** can plausibly lower the ground-state energy of adsorbed **5** relative to that of adsorbed **3**. Furthermore, the greater steric bulk and/or “stiffness” of the biphenyl moiety can plausibly inhibit disulfide formation for adsorbed **5** relative to that for adsorbed **3**, thereby increasing the transition-state barrier for the desorption of **5** relative to that of **3**.⁴⁸ Both reaction-limitation effects would predict greater stability for the SAMs derived from **5** relative to those derived from **3**.

The SAMs derived from **2** appear to be the least stable of the SAMs examined here (see the data in Table 5). With regard to diffusion limitation, the relatively low surface density of thiolate groups might permit facile diffusion for adsorbed **2** and thus rapid desorption from the surface. The apparent poor stability of these SAMs, however, might also arise statistically from the 2:1 ratio of tail group to thiol group for the adsorbate **2**; all other adsorbates possess a 1:1 ratio of tail group to thiol group. For the SAMs derived from **2**, the proposed desorption process removes four alkyl chains (i.e., tail groups) from the surface per disulfide bond formed; for the other adsorbates, the proposed desorption process removes only two alkyl chains per disulfide bond formed. Consequently, the enhanced loss of alkyl groups for adsorbed **2**, as judged by ellipsometry, would be interpreted to indicate poor stability for the SAMs derived from **2**.

Dependence of Activation Parameters on Chain Length. Previous desorption studies of SAMs on gold have found a relationship between chain length and SAM stability.^{12,45} For example, the desorption of normal alkanethiolate SAMs into hydrocarbon solvents suggested a stabilization of 0.2 kcal/mol per additional methylene unit.¹² Similarly, in the work reported here (see Figure 8), we find that the desorption of normal alkanethiolate SAMs **6** into isooctane indicates a stabilization of 0.3 ± 0.2 kcal/mol per additional methylene. Moreover, for the SAMs derived from **1**, we find a stabilization of 0.6 ± 0.2 kcal/mol per additional methylene, which is roughly twice that of the SAMs derived from **6**. While relative values of stabilization for **1** and **6** are consistent with the number of alkyl chains per type of adsorbate (i.e., two chains for **1** and one chain for **6**), the error associated with these values precludes the establishment of a concrete correlation.

Conclusions

The adsorption of compounds **1–6** onto the surface of gold affords densely packed and conformationally ordered monolayer films. The alkyl chains in the SAMs derived from **1** and **2** are slightly less crystalline than those in the SAMs derived from **3–6**. The low crystallinities of the former SAMs probably arise from conformational con-

(68) Broadhurst, G. J. *J. Res. Natl. Bur. Stand., Sect. A* **1962**, *66*, 241.

(69) Guryanova, E. N. *Q. Rep. Sulfur Chem.* **1970**, *5*, 113.

straints imposed by the aromatic ring, which initially directs the intramolecular alkyl chains in opposite directions and thereby adversely influences interchain packing. Desorption experiments in which the SAMs were exposed to hydrocarbon solvents at elevated temperatures revealed new insight into the structural parameters that dictate the thermal stabilities of SAMs on gold. The desorption profiles of SAMs of **1–6** exhibit two distinct kinetic regimes: an initial fast-desorbing regime followed by a slow/nondesorbing regime. The rate of monolayer desorption in both regimes increases with increasing temperature for all adsorbates. The rates of desorption in the fast-desorbing regime are probably limited predominantly by the rates of disulfide formation. The rates of desorption in the slow/nondesorbing regime are probably limited predominantly by the rates of diffusion of the adsorbates

on the surface. In both regimes, the SAMs derived from **1** appear to be the most robust when compared to the SAMs derived from **2, 3, 4, 5, and 6**.

Acknowledgment. The National Science Foundation (CHE-9625003, CAREER Award to T.R.L.) and the Robert A. Welch Foundation generously supported this research. The authors wish to thank Dr. Paul van der Heide for assistance with the XPS measurements.

Supporting Information Available: Experimental description of the methods used to prepare and characterize the SAMs and the thiol adsorbates. This material is available free of charge via the Internet at <http://pubs.acs.org>.

LA0115278